AD-A180 095 PORTABLE FUEL LEAK DETECTOR(U) AERODYNE PRODUCTS CORP 1/1
NORTH BILLERICA MA B D FIGLER JAN 87 AFWAL-TR-87-2021
F33615-86-C-2652

UNCLASSIFIED F/G 1/3 NL

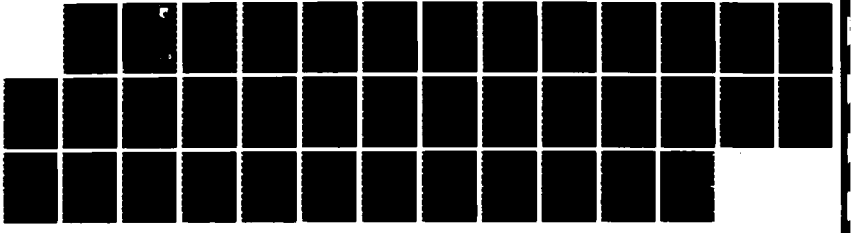

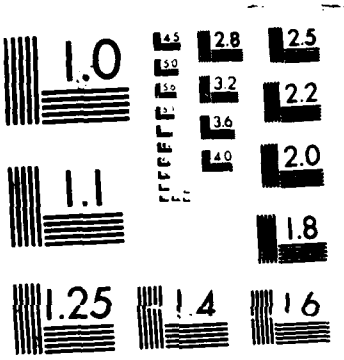

AFWAL-TR-87-2021

PORTABLE FUEL LEAK DETECTOR

Burton D. Figler

Aerodyne Products Corporation
76 Treble Cove Road
North Billerica, MA 01862

January 1987

Final Report for Period July 1986 - January 1987

Approved for Public Release; Distribution Unlimited.

AERO PROPULSION LABORATORY
AIR FORCE WRIGHT AERONAUTICAL LABORATORIES
AIR FORCE SYSTEMS COMMAND
WRIGHT-PATTERSON AIR FORCE BASE, OHIO 45433-6563

NOTICE

When Government drawings, specifications, or other data are used for any purpose other than in connection with a definitely Government-related procurement, the United States Government incurs no responsibility or any obligation whatsoever. The fact that the Government may have formulated or in any way supplied the said drawings, specifications, or other data, is not to be regarded by implication, or otherwise in any manner construed, as licensing the holder, or any other person or corporation; or as conveying any rights or permission to manufacture, use, or sell any patented invention that may in any way be related thereto.

This report has been reviewed by the Office of Public Affairs (ASD/PA) and is releasable to the National Technical Information Service (NTIS). At NTIS, it will be available to the general public, including foreign nations.

This technical report has been reviewed and is approved for publication.

MARIA D. RODRIGUEZ, Lt, USAF
Project Engineer

ROBERT G. CLODFELTER, Chief
Fire Protection Branch

FOR THE COMMANDER

ROBERT L. SHERRILL, Chief
Fuels and Lubrication Division
Aero Propulsion Laboratory

Accession For	
NTIS GRA&I	X
DTIC TAB	☐
Unannounced	☐
Justification	
By	
Distribution/	
Availability Codes	
Dist	Avail and/or Special
A-1	

If your address has changed, if you wish to be removed from our mailing list, or if the addressee is no longer employed by your organization, please notify AFWAL/POSH, WPAFB, OH 45433-6563 to help us maintain a current mailing list.

Copies of this report should not be returned unless return is required by security considerations, contractual obligations, or notice on a specific document.

19. ABSTRACT (Cont'd)

absorption cell. The device was calibrated with decane and can observe vapor down to 1 part per million. Fuels have the same infrared absorption band.

Measurements were made of the leak rate from an aluminum sheet with a 6 mil pinhole. The measurement cycle started by first wiping the surface, then placing the air sampling tube above the leak and drawing air through the absorption cell. The vapor in the absorption cell increased with time due to liquid spreading over the surface. A steady peak level was reached when the diameter of the liquid layer became larger than the diameter of the sampling tube. The leak rate is fit by the relation: Leak Rate = 13/t microliters per minute, where t is the time in minutes for the initial slope to reach the peak level. With continuous monitoring, leaks of less than 0.1 microliters/minute can be readily detected in bays. (This is less than one tenth the rate to produce a 1/4" spot in 6 minutes with the talc/dye method).

The performance of the breadboard indicates that a portable fuel leak detector, including batteries, would be 1"x2"x6" and weigh less than 1 pound.

DEVELOPMENT OF A PORTABLE FUEL LEAK DETECTOR

I. INTRODUCTION

Fuel leaks inside aircraft equipment bays and other dry bays are a potential hazard and pose a threat to the safety of aircraft systems and personnel. Given sufficient confinement time the vapors can reach combustible concentrations. It is desirable to detect the fuel leaks when the leakage is very small. Depending on the leakage rate, leaks must be repaired either immediately or during the scheduled normal maintenance cycle. In some situations, the high density of equipment stored inside the bay makes accessibility of certain regions very difficult and visual identification of leaks practically impossible. An ideal detection system would be suitable for both continuously monitoring individual areas within the bays for the presence of a leak, and for manually probing identified areas to determine the exact source of a leak.

The present method for determining the presence of a leak and the leak rate is to make visual observations of the presence of a leak and then to spray the region with talc powder containing a dye. Fuel from the leak wets the powder and causes the dye to turn red. The leak rate is determined by measuring the diameter of the red spot after 6 minutes. The initial detection of the leak is usually by visual observation of liquid fuel on the outside surface of the aircraft that is seeping from a bay.

Aerodyne proposes to detect fuel leaks by detecting the vapor which evaporates from the exposed fuel. The vapor is observed by means of its infrared absorption with a spectral correlation technique. This technique allows the detection of very small concentrations (down to 1 part per million) of fuel in bays. Also, it can accurately measure leak rates. This system permits the rapid detection of fuel in areas that are practically impossible to visually observe, and regions such as bays can remain closed during the inspection for leaks. The measurement of the leak rate is similar to that done with the powder. The region containing the leak is wiped clean and a vapor sampling tube is placed over the leak. Because of the high sensitivity,

the leak rate can be measured in seconds. The fuel vapor build up rate determines the fuel leak rate.

This report covers the work performed in this Phase I SBIR program. The next section presents predictions of the performance of this fuel leak detector. Section III presents quantitative measurements of leak rates with the Aerodyne technique. Section IV describes the spectral correlation technique that is used to measure the fuel vapor concentration. The final section summarizes the objectives and results of this program.

II. METHOD FOR DETECTING FUEL LEAKS

The fuel leak problem has two aspects: a need exists for a highly sensitive area monitor which can detect very low concentrations of fuel vapor which will exist some distance away from the source of the leak. A need also exists for a portable device which can be used to pinpoint the exact location of a leak and which has the ability to probe areas having poor accessibility. Figure 1 illustrates how fuel leaks in a dry bay can be detected. A sampling tube leading from the portable fuel leak detector, PFLD, is placed in a vent to the dry bay. A permanent installation of the fuel leak detector in the bay would provide continuous monitoring for leaks. Some of the fuel leaking into the dry bay area evaporates and the fuel vapor level builds up in the bay. The air in the bay containing the vapor is sampled with the fuel leak detector which has a high detection sensitivity. We shall show that fuel leak rates below 0.1 microliter/min in the bay can be detected even if the air in the bay changes only once every hour.

Once a fuel leak has been discovered, the next task is to determine the leak rate. Figure 2 illustrates the method for localizing and determining the leak rate. The dry bay area is open and the air sampling tube is rapidly moved over surfaces with potential leaks to locate the region with the highest fuel vapor level. The region containing a leak is dried with a cloth and the vapor evaporated from the liquid leaving the hole is measured. This is illustrated in Figure 3, the vapor concentration in the sampled air is shown versus time. The 1/4" diameter sampling tube is placed over (but in contact with) the leaking region; air containing fuel vapor evaporated from the liquid fuel is pumped through the tube. The time in Figure 3 starts when the surface is wiped clean. The liquid leaks at a constant rate and a liquid layer spreads over the surface. The signal increases until the liquid layer diameter exceeds 1/4", i.e. becomes larger than the sampling tube. Then the signal becomes constant because the evaporation from the liquid reaches a steady state over the area of the sampling tube. The response of the fuel leak detector for different leak rates is illustrated in Figure 4. Leak rates in which the spot diameter reaches a 0.25, 0.75, 2.5, and 6 inches in six minutes illustrates the range of operation of the system for leak rate measurements.

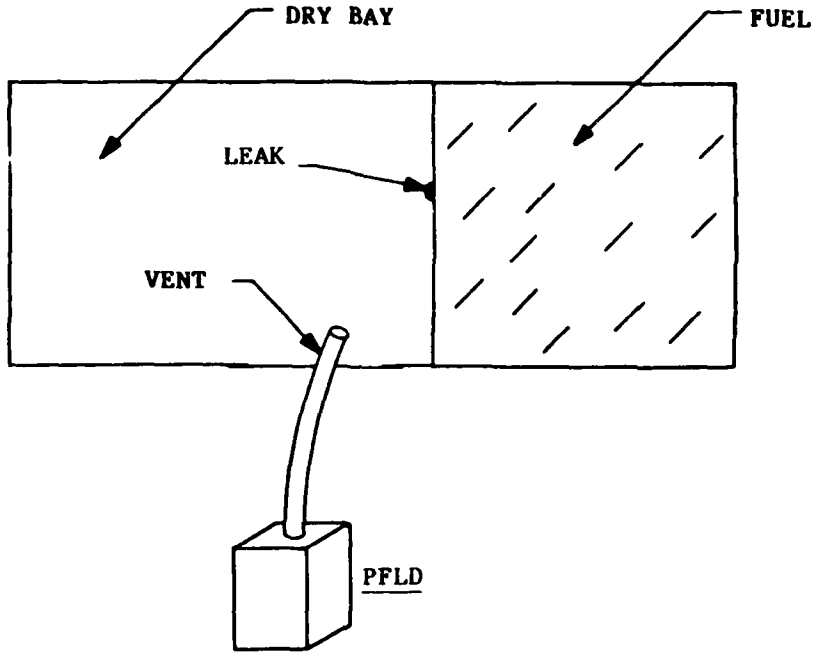

Figure 1. Fuel Leak Detection System

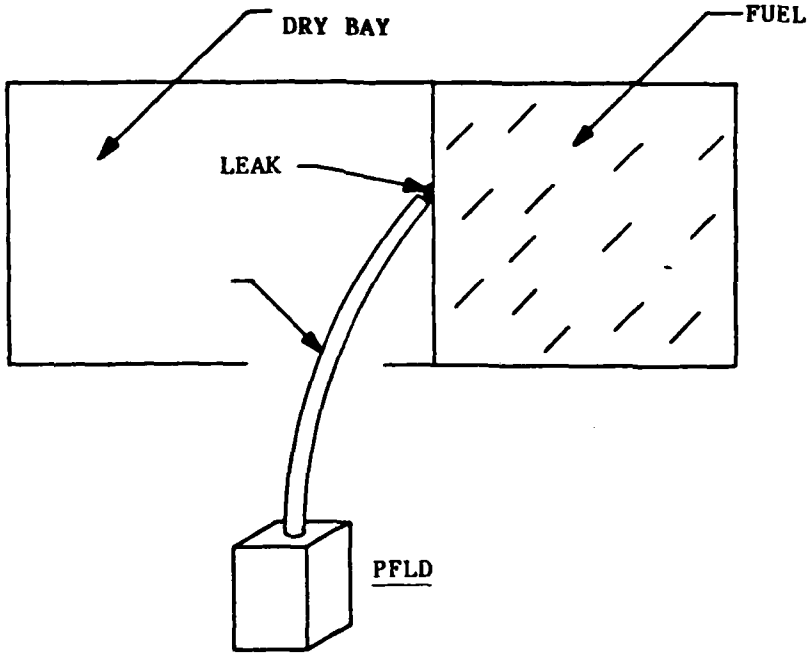

Figure 2. Fuel Leak Localization and Leak Rate Measurement

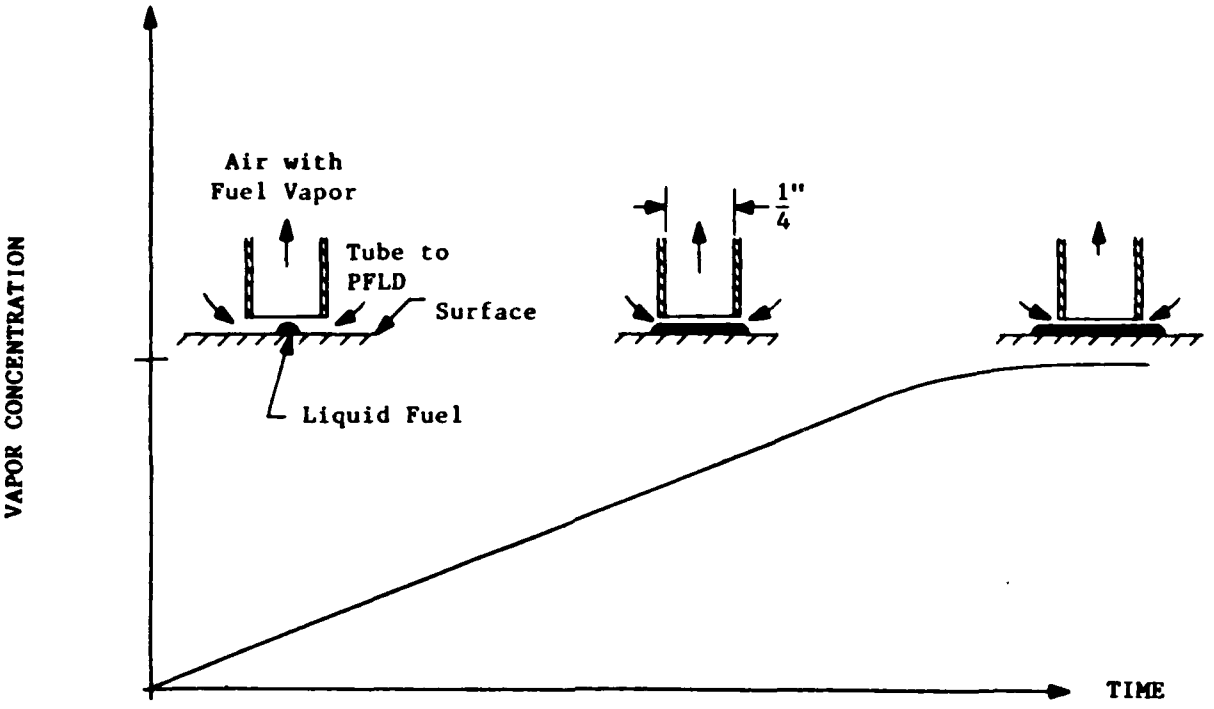

Figure 3. Leak Rate Measurements with Portable Fuel Leak Detector, PFLD

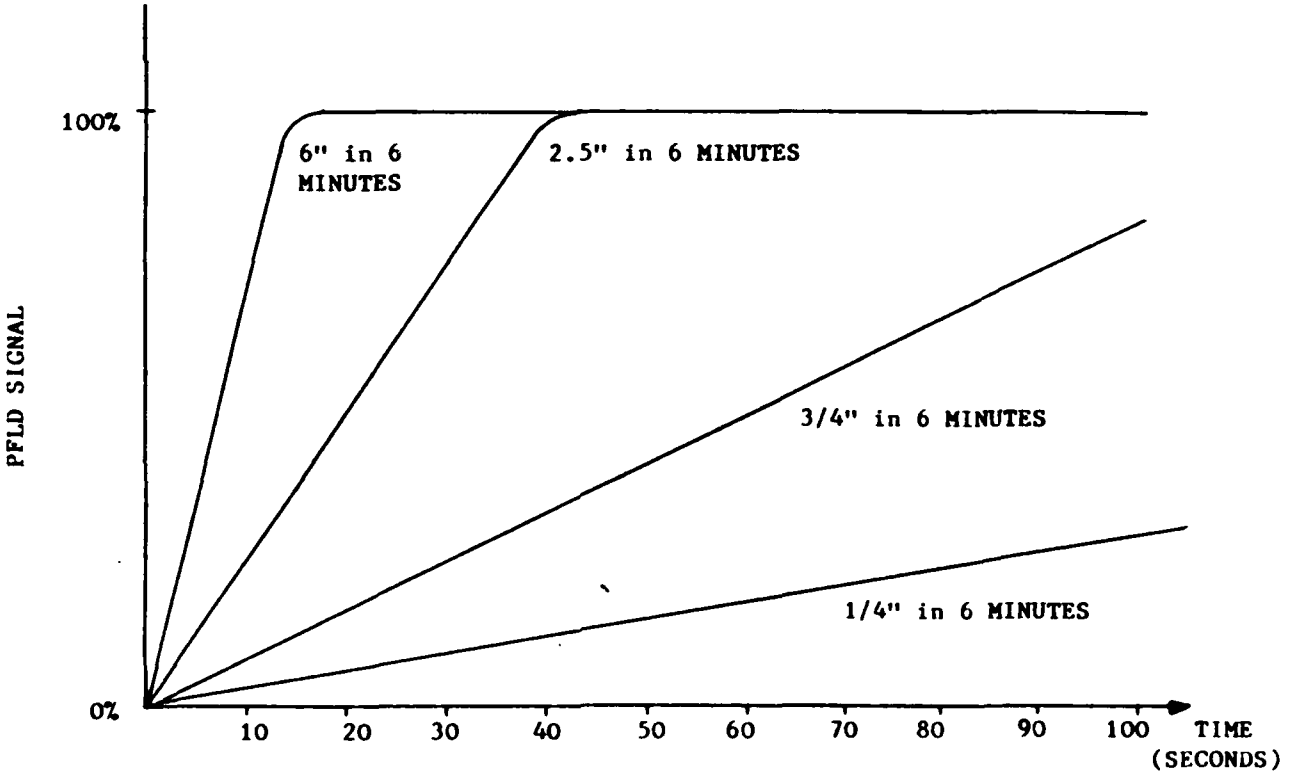

Figure 4. The PFLD Signal Versus Time for Fuel Leak Rates that Produce Spot Diameters of 1/4, 3/4, 2.5 and 6 Inches in 6 Minutes

The leak rate is determined by measuring the slope of the curve. For example, measurements of leak rates larger than 0.75 inch spot diameter after six minutes can be made in 10 seconds; smaller leak rates can be measured in 100 seconds. The readout can present the leak rate in μℓ/min or the equivalent spot diameter after six minutes. We now present the calculations that produced the curves shown in Figure 4.

Predictions Of Fuel Leak Rate

The fuel leak rate measurement using the Aerodyne system is based on the following analysis. The measurement arrangement is shown in Figure 3. A 0.25 inch tube is placed over, but not in contact with, the surface. Air flows over the liquid layer and is pumped through the tube to the fuel leak detector. The flow geometry is illustrated in Figure 5.

A layer at the surface of the liquid is the region containing fuel vapor. The vapor concentration in the layer varies from the vapor pressure at the liquid surface to zero at the boundary layer air interface. The letters in Figure 5 have the following meaning:

S = Layer Thickness, cm
t = Liquid Fuel Layer Thickness, cm
D = Fuel Spot Diameter, cm
u = Air Flow Velocity, cm per second

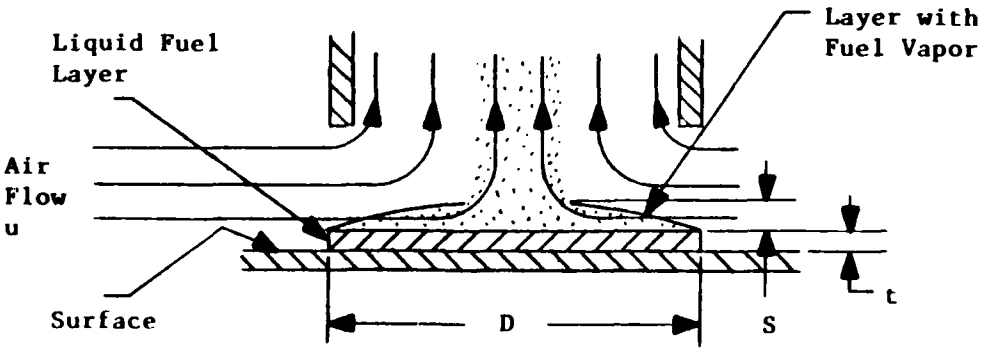

Figure 5. Flowfield Over Liquid Fuel Layer

The layer thickness, S, is approximately

$$S = (mDa/2u)^{1/2},$$

where m = mean free path for molecular collision, cm; and a = speed of sound, cm per second.

The amount of fuel vapor transported by the flow, V_f, is then given by

$$V_f = 0.5\ PuDS = 0.5\ PD^{3/2}(mau/2)^{1/2},$$

where V_f = is in cm^3/sec; P = fuel vapor pressure in parts per million.

At 68 ^oF (20 ^oC), the vapor pressure of decane ($C_{10}H_{22}$), P, is approximately 1700 ppm.

The conversion from fuel gas volume to fuel liquid volume is

1 cm^3 of vapor (at 68 ^oF and 1 ppm) = 7×10^{-6} mm^3 of liquid.

The liquid volume evaporated (transported by the flow) V_ℓ, in mm^3/min or $\mu\ell/min$, becomes

$$V_\ell = (60)(7 \times 10^{-6})(0.5)\ PD^{3/2}(mau/2)^{1/2}$$

Assuming the following values: u = 150 cm/sec, a = 30,000 cm/sec, m = 6×10^{-6} cm, and D = 0.635 cm = 1/4 in, then

$$(mau/2) = (6 \times 10^{-6})(3 \times 10^4)(150)/2 = 13.5\ cm^3/sec^2$$

and

$$V_\ell = (0.00021)(1700)(0.635)^{3/2}\ (13.5)^{1/2} = 0.66\ mm^3/min\ (\mu\ell/min)$$

For a liquid fuel layer thickness, t, of approximately 0.15 mm (6 mils), a 0.8 $\mu\ell/min$ fuel leak rate will produce a liquid fuel 1/4" diameter spot in

six minutes.

For a 1/4" tube diameter, an air flow in the tube of 150 cm/sec and fuel leak rates up to 0.8 μℓ/min the liquid fully evaporates before growing to 1/4" diameter. For larger leak rates, the liquid layer does not completely evaporate.

Thus, for fuel leak rates below 0.8 μℓ/min, the PFLD signal levels off before reading the level shown in Figure 5. For fuel leak rates above 0.8 μℓ/min, the PFLD signal increases until the liquid fuel spot diameter is slightly larger than the sampling tube diameter. During the period of time when the PFLD signal increases with time, the rate of change of the PFLD signal is proportional to the fuel leak rate.

The Boundary Layer Thickness, S, can be determined by using values of the above example

$$S = (mDa/2u)^{1/2} = [(6 \times 10^{-6})(0.635)(3 \times 10^{4})/2(150)]^{1/2} = 0.019 \text{ cm.}$$

For a PFLD tube standoff distance of 1 mm, the tube standoff distance is 5 times the boundary layer thickness.

Leak Detection In Bays

Leaks can be detected in a bay using the geometry shown in Figure 1. The PFLD sensitivity to fuel vapor is 1 ppm. Thus, measurements can be made when the fuel vapor is 1 ppm in the bay.

The fuel volume conversion from gas (at 68 ^{o}f and 1 ppm) to liquid is

(7×10^{-6}) μℓ liquid = 1 cm^3 gas or 0.2 μℓ liquid = 1 ft^3 gas

If the air residence time in the bay is 1 hour, then the PFLD has the ability to detect leak rates as low as

0.2/60 = 0.003 (μℓ/min) per cubic foot of dry bay.

In summary, the Aerodyne Portable Fuel Leak Detector possesses the ability to detect fuel confined to bays for leak rates well under 0.1 μℓ/min. Localization and leak rate measurement can be achieved for fuel leak rates below 1 μℓ/min.

III. MEASUREMENTS OF FUEL LEAK RATES

A breadboard fuel leak detection system was constructed, and preliminary fuel leak measurements were obtained. The objective in this Phase I program is to show how measurements of fuel leaks can be made with the system. Detailed fuel leak measurements for different fuels and surface configurations are beyond the scope of this Phase I program, and would be performed in a follow-on Phase II program. The experimental arrangement is shown schematically in Figure 6A. Decane was used to simulate fuel. Decane vapor at different concentrations was fed into an absorption cell. The infrared transmission of the cell produced readings depending on the decane concentration. The absorption measurements were made as follows. An infrared glowbar source produced the radiation. Light from the glowbar went through a multipass absorption cell and then to a detector. A chopper alternated allowed light to pass alternately through one filter and then the other. The signal from the detector was amplified and sent to a phase-locked amplifier which was phase locked with the chopper. The output was read on a voltmeter. The concentration of decane in the absorption cell was controlled with a flow system. Nitrogen gas flowed into two paths, one with pure nitrogen, and the other with nitrogen bubbling through decane. The bubbles were small enough so that the nitrogen became saturated with decane vapor. The flow through the two systems was determined with flowmeters. Let V_N be the pure nitrogen flow rate, and V_D be the nitrogen flow rate through the decane bubbler. The concentration of decane vapor in the absorption cell is given by

$$C = P \frac{V_D}{V_N + V_D}$$

P is the vapor pressure of decane at 68 ^{o}F; the vapor pressure is

$$P = 1700 \text{ ppm}$$

The flows in the decane bubbler were varied, and the range of values of the flows were

$$V_N = 0.8 \text{ cfm}; \; V_D = 0 \text{ to } 0.1 \text{ cfm}$$

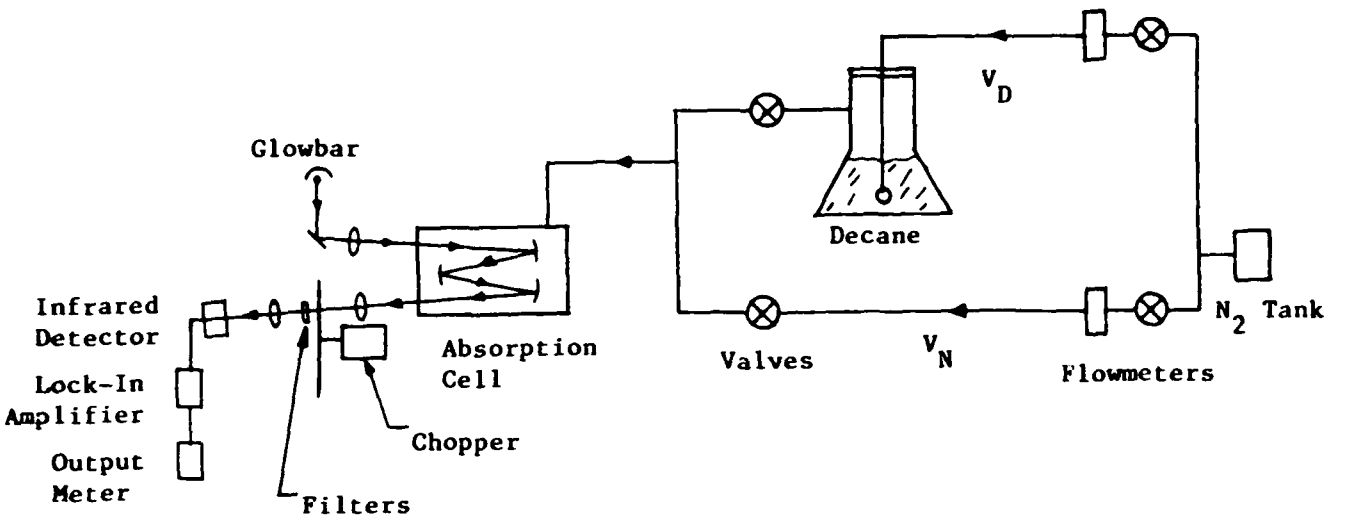

Figure 6A. Apparatus for Calibrating PFLD System with Decane Vapor

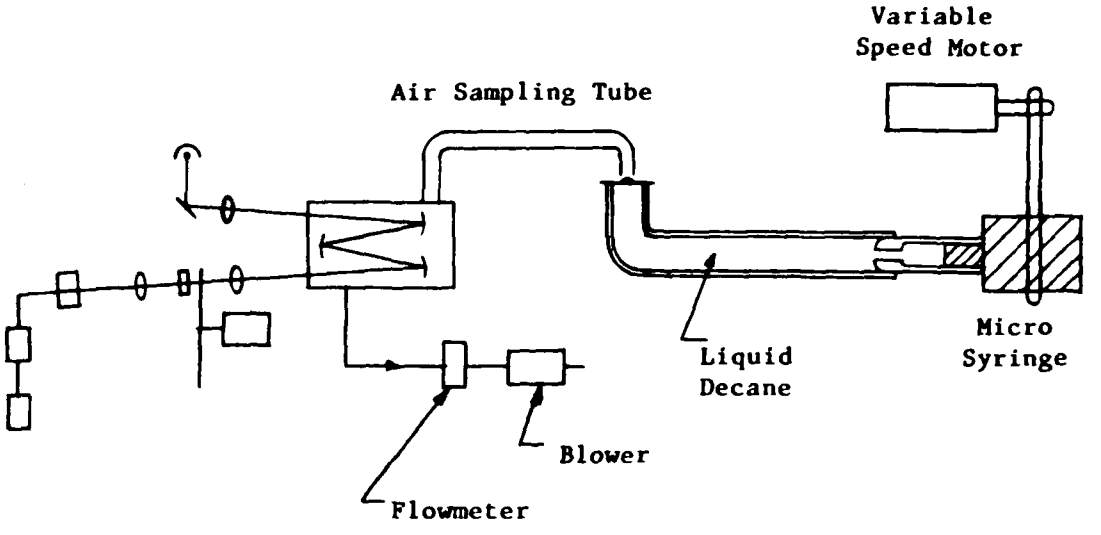

Figure 6B. Apparatus for Measuring Decane Leak Rates

The output of the lock-in amplifier in millivolts as a function of the decane partial pressure in ppm is shown in Figure 7. The absorption cell had 0 to 190 ppm of decane in nitrogen. Note that the curve is linear; thus the output of the lock-in amplifier is proportional to the concentration of decane. The relation between the signal and the decane concentration in ppm, C, is given by

Signal [millivolts] = 0.22 C

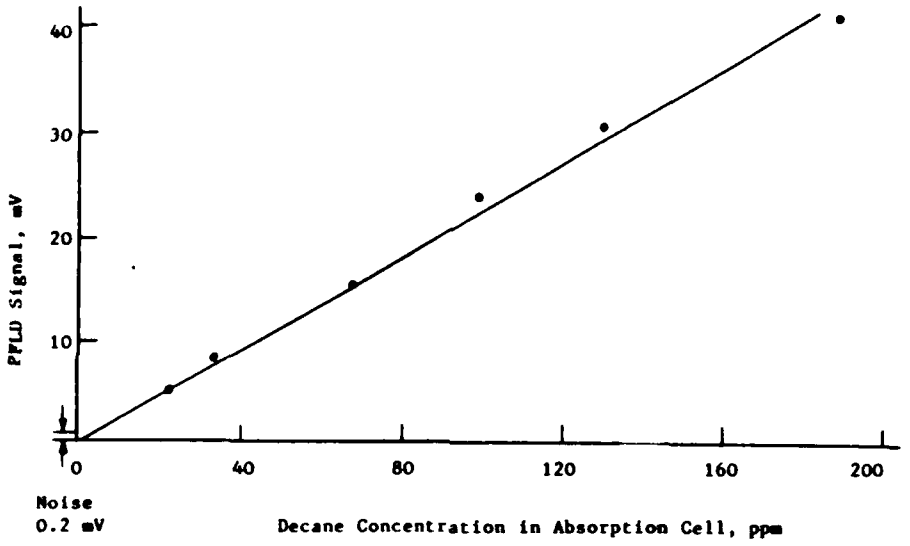

Figure 7. The Fuel Leak Detector System Calibration with Decane Vapor

In the follow-on Phase II program the linear results would be obtained for the different fuels. The noise of the lock-in amplifier is 0.2 mV and this corresponds to a pressure of approximately 1 ppm. Thus, this system is linear to over 190 ppm and has a noise level of about 1 ppm.

The apparatus was then used to measure the decane leak rate. Similar results are expected for the different fuels. The experimental arrangement is shown in Figure 6B. The same optical and detection system is used. However,

the flow system was changed. Tygon tubing, 6 mm I.D., was connected to the absorption cell. The other side of the absorption cell was connected to a blower, and air was sucked through the tygon tube, the absorption cell and the blower. A flowmeter set the flow rate at 0.1 cfm. At this flow rate, the flow took 0.4 seconds in the tygon tube and 3 seconds in the absorption cell.

The apparatus for producing a controlled decane leak rate is also shown in Figure 6B. An aluminum plate with a 6 mil hole was used for the leaking surface. The plate was connected with a tube to a microsyringe in which one turn of the syringe was ten microliters. A variable speed motor was coupled to the syringe with an "O" ring. The leak through the hole in the aluminum was produced by turning the microsyringe at a constant rate.

The tygon tubing connected to the absorption cell is placed in contact with the aluminum surface, the edge is notched so that only four points of the tygon touched the surface, the rest permitted flow across the surface. The notches are approximately 1 mm deep. Measurements were made of the output of the lock-in amplifier as a function of time for different leak rates. The results are shown in Figure 8. Zero time is at the start of the decane liquid leak. The decane concentration in the absorption cell is plotted versus time for three leaks rates, 3.5, 7.3, and 10.0 microliters per minute. Note that the curves rise linearly and then saturate at approximately 35 ppm of decane in the absorption cell. The time to reach the saturation level with the initial slope is indicated with dashed curves in Figure 8, and equals 4.5, 1.7, and 1.3 minutes for the 3.5, 7.3, and 10.0 microliters per minute leak rate. These results are shown in Figure 9, where the time, t_i, to reach the peak with the initial slope is plotted as a function of the leak rate in microliters per minute. The data shown in Figure 9 can be fit with the relation

$$\text{(leak rate)} = 13\ \mu\ell/t_i$$

$$\text{where } (1/t_i) = \frac{1}{S_p}\left(\frac{\Delta S}{\Delta t}\right) = \frac{\text{initial slope}}{\text{peak signal}}$$

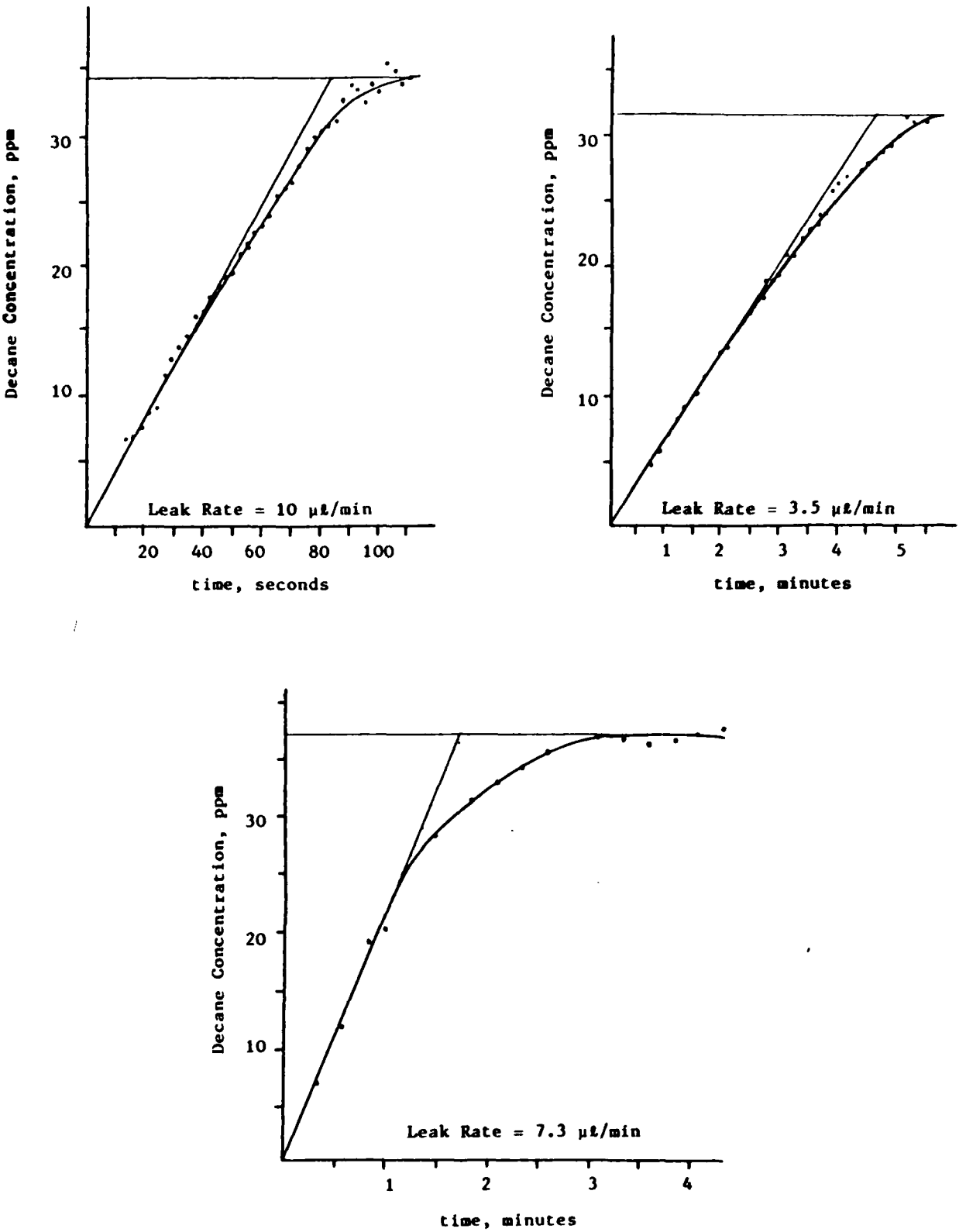

Figure 8. Decane Leak Rate Measurements. Decane Concentration (in ppm) in the Absorption Cell Versus Time

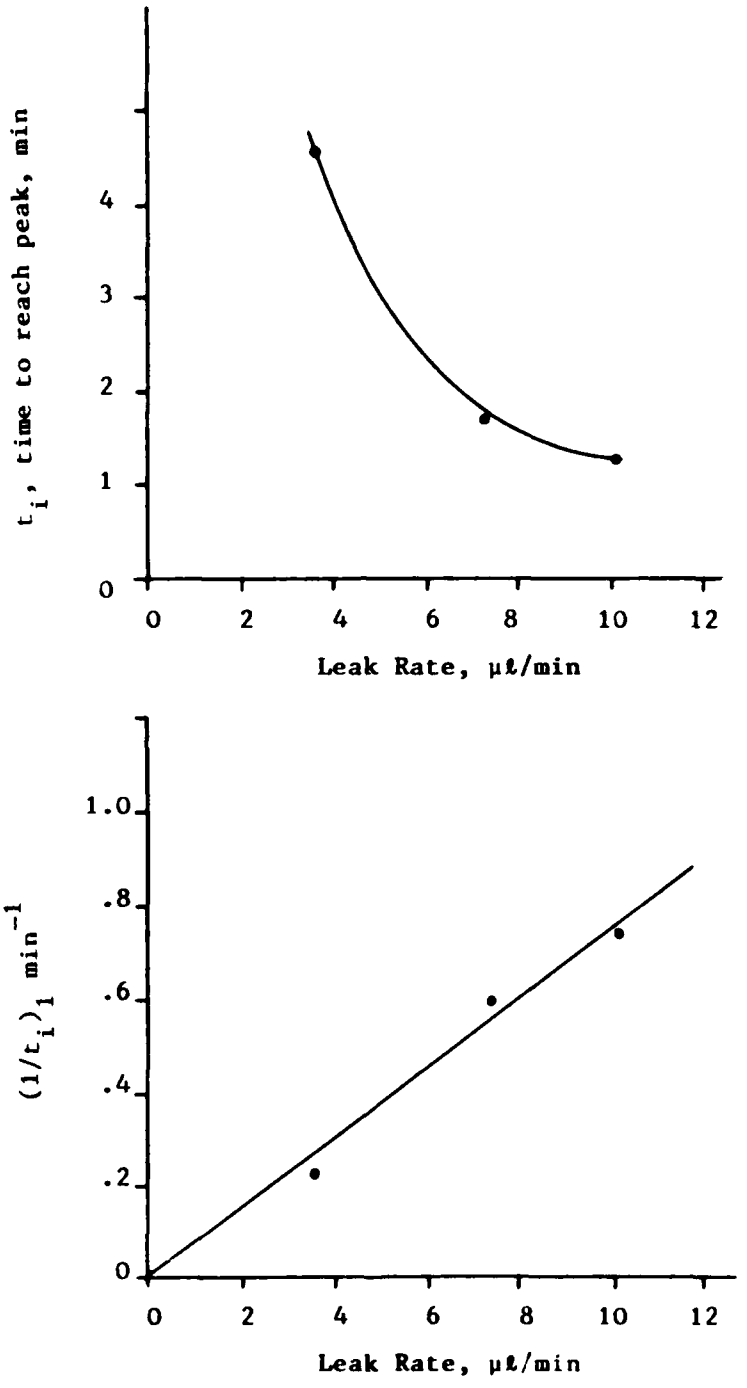

Figure 9. Time to Reach Peak Level, t_i, and $(1/t_i)$ Versus the Decane Leak Rate

where S is the signal output of the lock-in amplifier, and S_p is the peak level. Thus, the leak rate can be determined by measuring the time to reach the saturation level.

The absorption cell calibration data as well as the leak rate measurements are preliminary and illustrate the method for determining leak rates. A major task in the Phase II program would be to establish measurement techniques for different fuels and different types of surfaces. The calibration constants for different fuels would be incorporated into the electronics. The output meter would present: (1) the fuel vapor concentration, or (2) the leak rate in microliters/minute.

IV. FUEL LEAK DETECTION SYSTEM

Technical Background

The spectral correlator concept is illustrated in Figure 10. A glowbar rod heated up to 1500 K is used for the infrared source. Light from the glowbar is focused in a gas absorption cell, refocused on a pair of filters, and finally refocused on a single detector. The gas absorption cell is filled with sampled gas containing wet or dry air with varying concentrations of fuel vapor. Half of the glowbar rod is focused on Filter 1 and the other half is focused on Filter 2. A chopper wheel alternately exposes one half or the other half of the glowbar. Thus, alternately Filter 1 and Filter 2 are illuminated. Light from both filters is focused on the infrared detector. The detector alternately sees radiation from Filters 1 and 2. The detector signal is processed with a lock-in amplifier for the difference in the light intensity transmitted through the two filters. The difference signal is integrated for about one second. We shall show that the difference signal is proportional to the fuel vapor concentration.

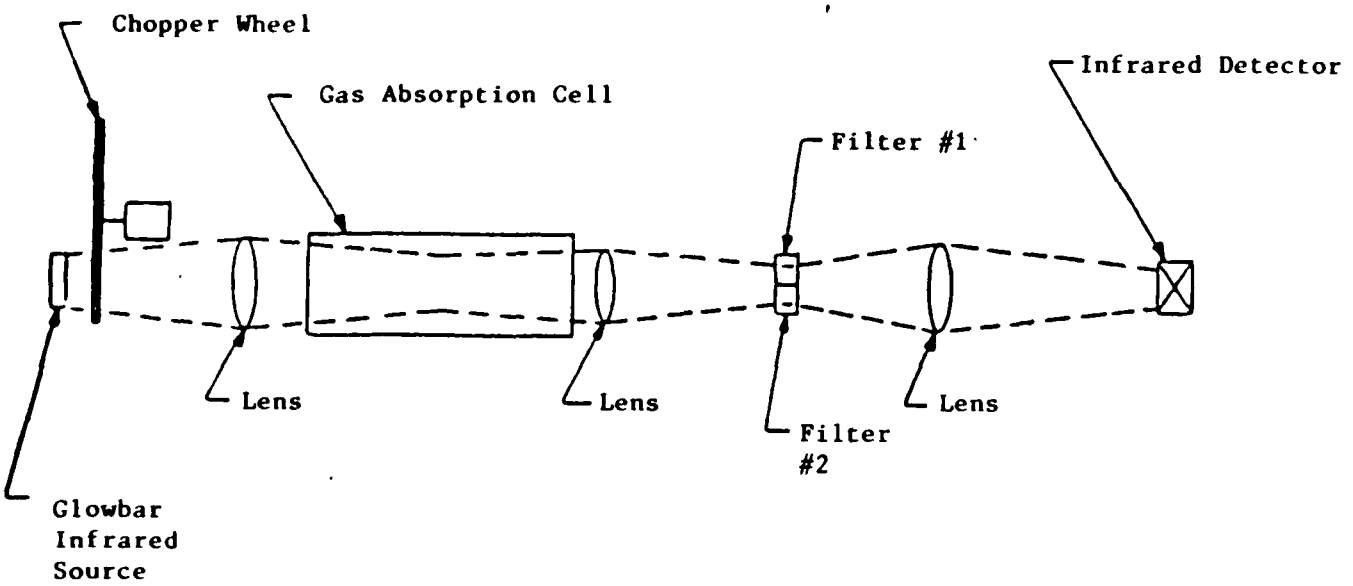

Figure 10. Schematic of Infrared Spectral Correlation System

We now describe the operation of this system and the selection of the infrared Filters 1 and 2.

General Concepts

The objective is to measure trace levels of jet fuel vapor in air using the infrared absorption of the vapor. By comparing the absorption in two spectral regions, a differential measurement can be made which eliminates the need for a highly stable, calibrated infrared source. However, at the wavelengths with significant fuel vapor absorption, there can also absorption by air molecules, in particular, water vapor. The water vapor content of air is highly variable. Fortunately, the water vapor absorption is weak in the spectral region where the fuel vapor absorption is strong; 1 part per million of fuel vapor in air has stronger absorption than water vapor absorption at 100% relative humidity at 73 ^{o}F. Thus, the design of the system does not have to consider water vapor absorption.

Analysis

Consider the two spectral bands for Filters 1 and 2. The observed signals S_1 and S_2, through Filters 1 and 2, due to fuel vapor concentration C are

$$S_1 (C) = \int_1 I_L R\tau_1 \exp[- \alpha C \ell] d\lambda \quad (1)$$

$$S_2 (C) = \int_2 I_L R\tau_2 \exp[- \beta C \ell] d\lambda \quad (2)$$

where α and β are the fuel vapor absorption coefficients in spectral bands 1 and 2. ℓ is the optical path length in the absorbing medium; I_L is the lamp intensity; R is the response of the detector, and τ_1 and τ_2 are the transmission of the optical trains, including Filters 1 and 2, respectively.

We choose the bands so that the following conditions are satisfied:

- The signals are the same with no absorption in the cell,

$$S_1 (C = 0) = S_2 (C = 0) \tag{3}$$

$$\int_1 I_L R\tau_1 d\lambda = \int_2 I_L R\tau_2 d\lambda$$

o The absorption by the fuel vapor is much larger in spectral region 1 than in region 2,

$$\alpha >> \beta \tag{4}$$

If the absorption is small, then Equations 1 and 2 become

$$S_1 (C) \approx \int_1 I_L R\tau_1 [1 - \alpha C \ell] d\lambda \tag{5}$$

and

$$S_2 (C) \approx \int_2 I_L R\tau_2 [1 - \beta C \ell] d\lambda. \tag{6}$$

The difference signal ΔS becomes

$$\Delta S = S_1 (C) - S_2 (C)$$

$$= [S_1 (C = 0) - S_2 (C = 0)] - C \ell \left[\int_1 I_L R\tau_1 \alpha \, d\lambda - \int_2 I_L R\tau_2 \beta \, d\lambda\right]. \tag{7}$$

Applying the conditions presented in Equations (3) and (4), we obtain

$$\Delta S = C \ell \int_1 I_L R\alpha\tau_1 d\lambda \tag{8}$$

Equation (8) is the final result. Note that the difference signal ΔS is directly proportional to the fuel vapor concentration C . Thus, the spectral correlator system can measure fuel vapor directly.

Selection of the Infrared Filters

We now apply the spectral correlator technique to the measurement of small concentrations of jet fuel vapor. We require that the spectral region for Filter 1 has strong infrared absorption by the fuel vapor. Figure 11 shows the spectral transmission of octane, decane and tridecane (typical components of jet fuel) in the region from 2.5 to 5 μm. The strong absorption band is between 3.35 and 3.5 μm for all three species. Figure 12 shows a detailed transmission spectrum for decane in the 3 to 4 μm region. Thus, we select Filter 1 to transmit around 3.40 μm (2940 cm^{-1}).

The main atmospheric absorption is by water vapor. Figure 13 shows the transmission of water vapor in saturated air at 20 ^{o}C. Since in most field situations the concentration of water vapor is unknown, the water vapor uncertainty could be the limitation to the lowest measurable jet fuel vapor concentration. Fortunately, in the spectral band for decane absorption, the H_2O absorption is less than 0.003, below the detection sensitivity of the system. Filter 2 is selected so that both the decane and the water vapor absorption are small in its spectral passband. We select the band from 3.5 to 3.7 μm.

Decane Absorption Coefficient

Experimental measurements of the absorption of decane gas were carried out by APC, using the experimental arrangement shown in Figure 14.

Light from a glowbar infrared source, S1, is made parallel with the mirror, M1, the light traversed a 24" absorption cell and is focused with mirror, M3, on a monochromator. The light exiting the monochromator is focused with mirror, M4, on an infrared detector. The light is chopped with the rotating chopper blade, C1. The output signal of detector, D1, is fed into a lock-in amplifier synchronized with the chopper. The output of the locked-in amplifier goes to a chart recorder. The gas in the absorption cell is controlled with a flow device. High pressure nitrogen is divided into a line going directly to the absorption cell, and a line bubbling through decane and then to the absorption cell. The flow rates of nitrogen in the two lines

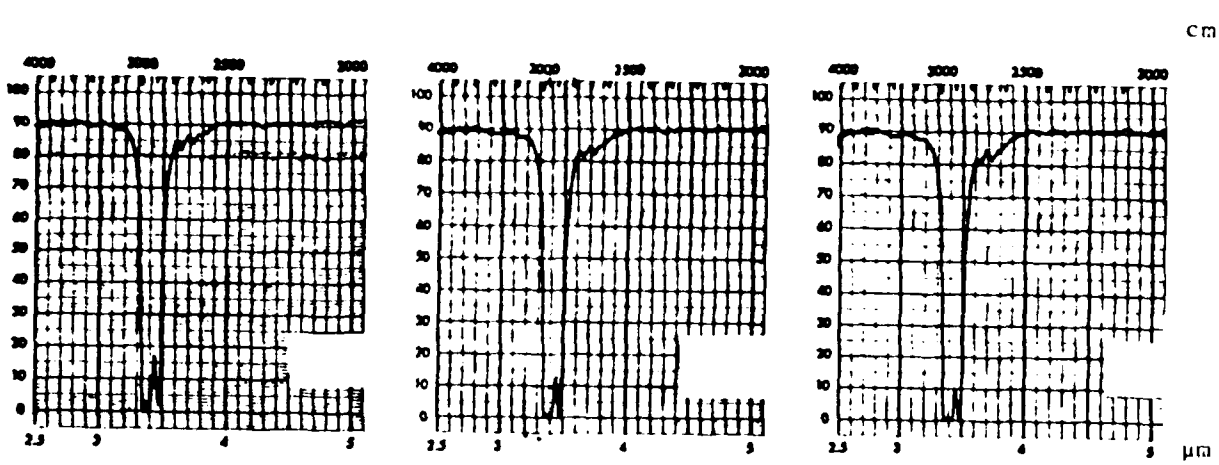

Octane
$CH_3\ (CH_2)_6\ CH_3$

Decane
$CH_3\ (CH_2)_8\ CH_3$

Tridecane
$CH_3(CH_2)_{11}\ CH_3$

Figure 11. Infrared Absorption Spectra for Octane, Decane and Tridecane

Note: Absorption at 3.4 μm is similar for these species

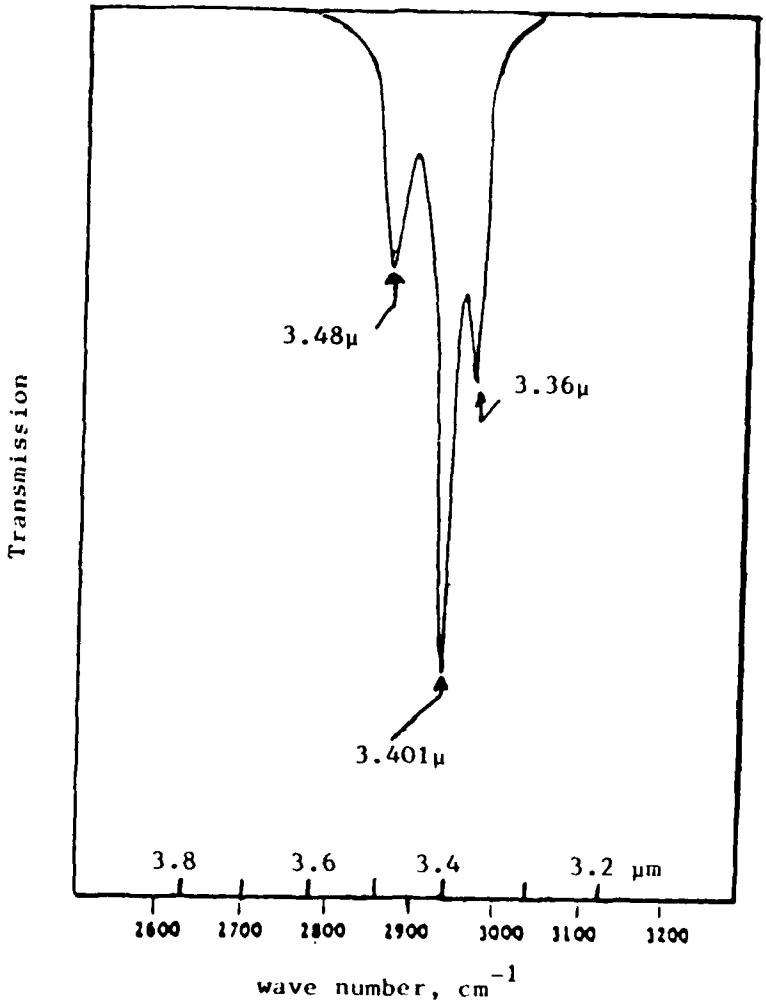

Figure 12. Transmission of Decane Vapor

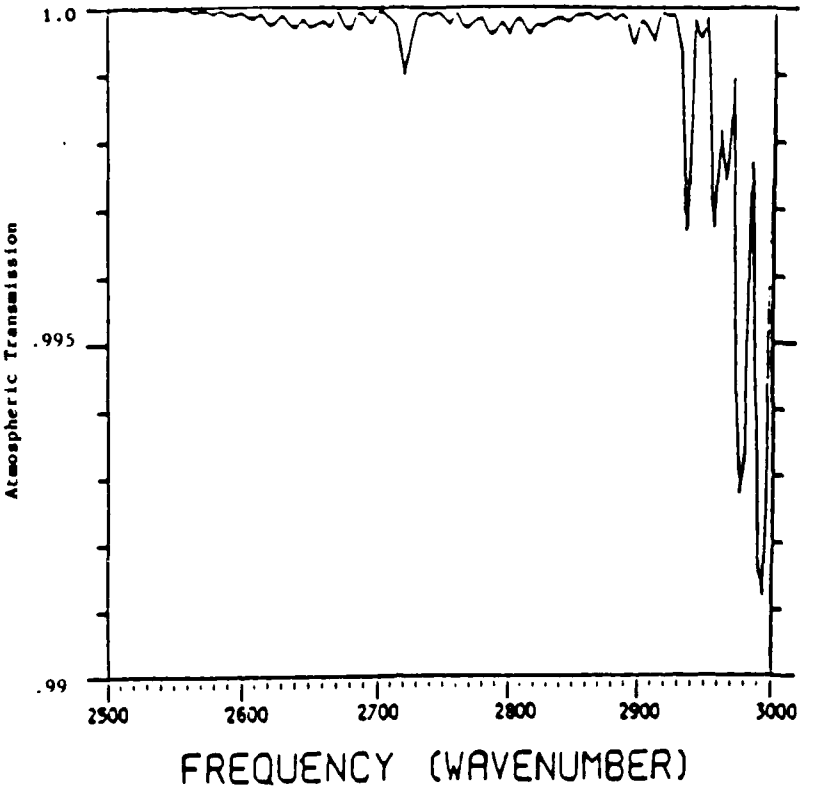

Figure 13. Atmospheric Transmission over 1m Path with Saturated Water Vapor at 20 °C (35 parts per thousand)

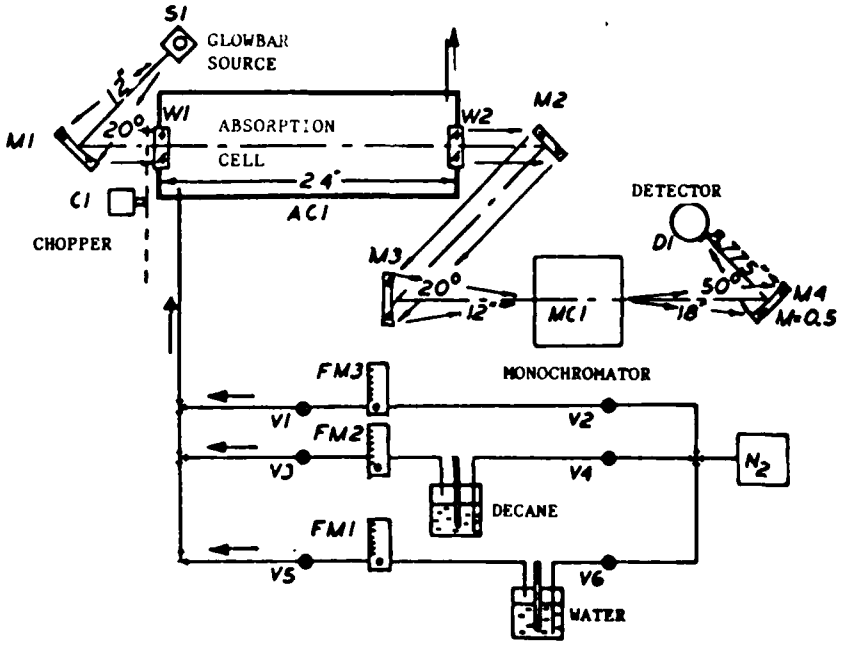

Figure 14. Arrangement for Measuring Decane Absorption

are set with flowmeters. The decane absorption versus wavelength is obtained by moving the monochromator grating. The results of measurements with 300 ppm decane in the absorption cell are shown in Figure 15. There are three lines at 3.36, 3.40, and 3.48 micrometers. The transmittance at the peaks of these lines is 0.65, 0.47, and 0.74. The selection of the filter to measure decane uses the most absorbing portion of the spectrum.

The absorption coefficient, α, is determined from the following equation for transmission through a gas.

$$T = I/I_o = \exp(- C\alpha\ell)$$

T = Transmission
I = Intensity of radiation emerging from gas path
I_o = Intensity of radiation entering gas path
C = Concentration (Atmospheres)
ℓ = Path Length (Centimeters)
α = Absorption Coefficient ($Atm^{-1}Cm^{-1}$)

The experimental parameters for the decane spectrum were:

Ambient Temperature:	20 ^{o}C (nominal)
Decane Concentration, C	300 ppm = (3×10^{-4} Atm)
Path Length, ℓ	61 cm = (24 inches)

The values for α are: 24, 41, and 16 atm^{-1} cm^{-1} at 3.36, 3.40, and 3.48 µm, respectively.

Using the value of the absorption coefficient at 3.40 µm, the transmission can be readily calculated for other path lengths and decane concentrations. The table below provides values of transmission for a 40 inch path length.

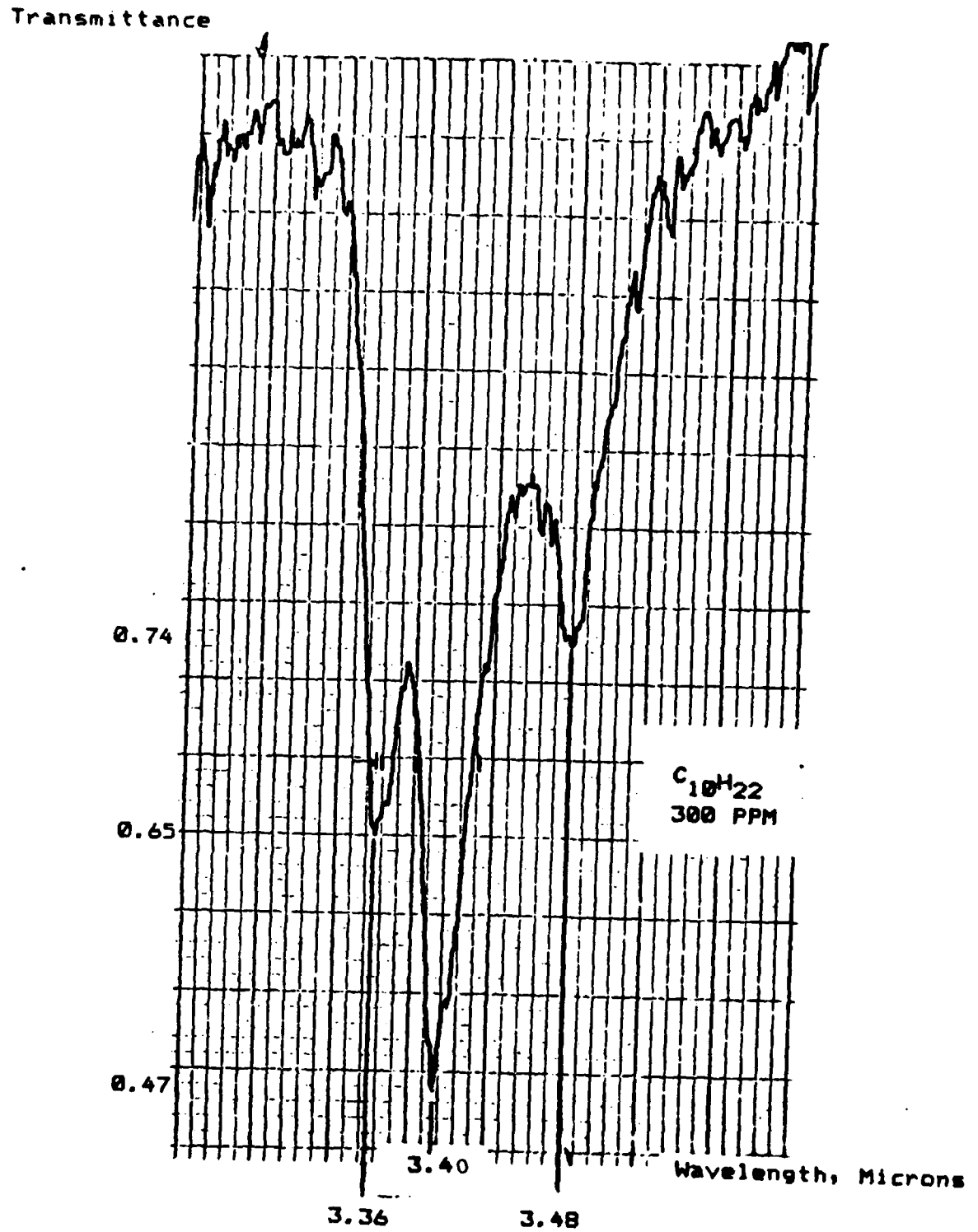

Figure 15. Experimental Decane Absorption Spectrum

Path Length (inches)	Concentration (ppm)	Transmission	Absorption
40	1	0.997	0.0025
40	10	0.975	0.0250
40	100	0.779	0.250

The sensitivity of the breadboard system to be described later can observe an absorption of 0.003 which corresponds to 0.8 ppm decane.

V. OPTICAL SYSTEM DESIGN

The Portable Fuel Leak Detector (PFLD) optical system design is illustrated in Figure 16. The glowbar source (S1) is imaged 1:1 onto the entrance of the absorption cell (AC). The glowbar dimensions are approximately 0.060" (H) x 0.200" (W).

Lens L1 images the source onto the slit. L1 has a 1" focal length and an effective aperture of 0.25". The object and image distances of L1 are both 2", so that the lens operates at f/8.

The absorption cell mirrors, M1, M2, and M3 all have 4" radii of curvature. M1 is a nominal 1" in diameter, with M2 and M3 having a nominal diameter of 0.5". M2 and M3 thus operate at an effective f/# of f/8.

Lens L2 relays the output image of the absorption cell at 1:1 onto a chopper (C1). L2 has a focal length of 1" and an effective diameter of 0.25". The object and image distances are both 2" so that the lens operates at f/8.

L3 serves as a field lens. It has a focal length of 1" and is located just after the pair of filters, F1 and F2, and the chopper wheel. It is nominally 2" from both L2 and the PbSe detector (D1) so that it images L2 onto D1. For practical reasons, L3's object distance is slightly greater than 2" (approximately 2.25") and its image distance is slightly less than 2" (approximately 1.80"). Its effective diameter is slightly in excess of 0.25".

D1 is 0.6 cm x 0.6 cm in size and transduces the received infrared power into an electrical signal. The output of the detector is amplified and then goes to a lock-in amplifier.

The filters F1 and F2 are each 0.5 cm x 0.5 cm area and are in contact making a filter pair 0.5 cm x 1.0 cm. The chopper wheel C1 alternately covers F1 and F2. The spectral response of the filters is shown in Figure 17. A knife edge partially covers filter F2 and is adjusted for "zero" difference signal with no absorption in the White cell to satisfy the conditions of Equation (3).

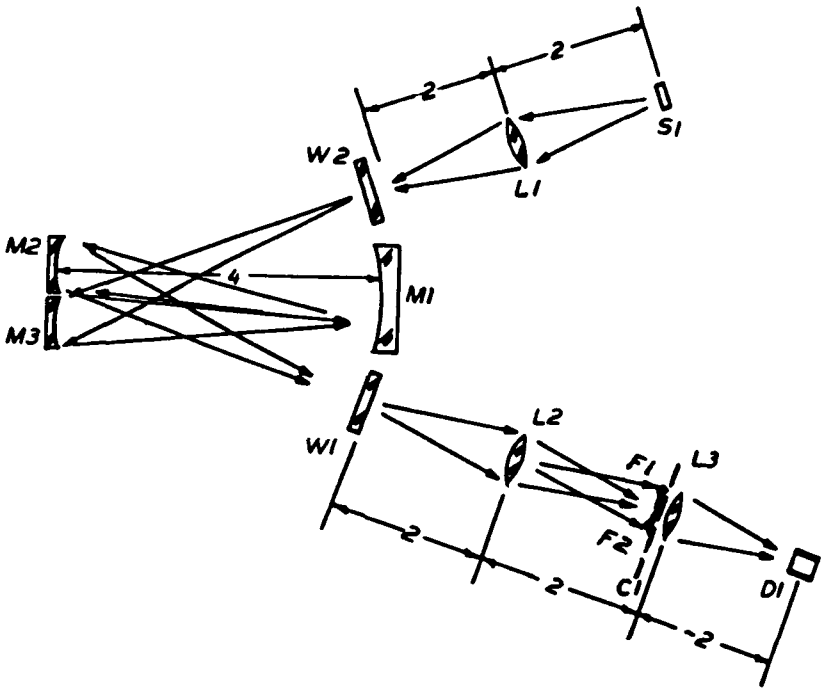

Figure 16. PFLD Optical Schematic

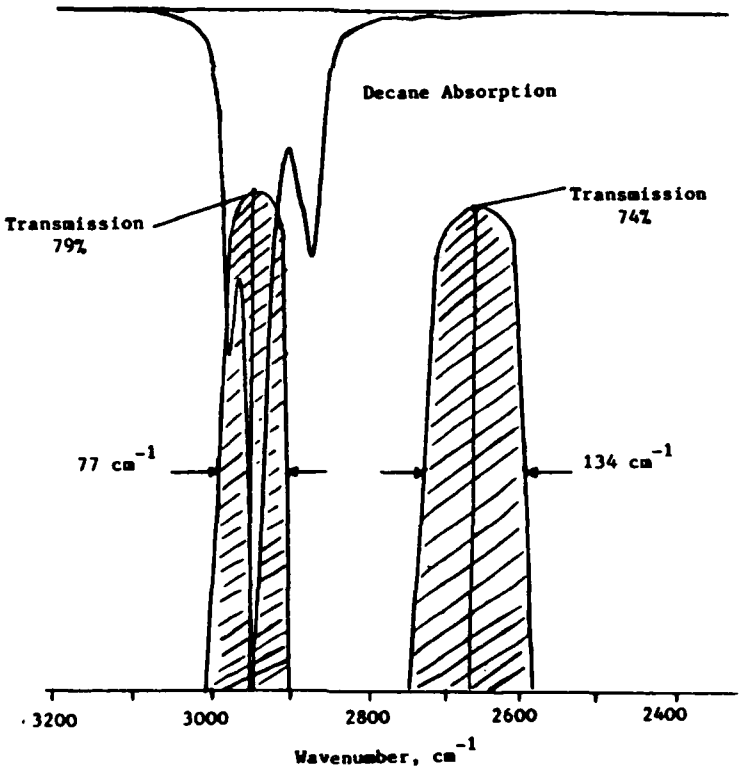

Figure 17. Filter F_1, F_2 Transmission

In order to make absorption measurements of air samples the White cell is enclosed. Windows W1 and W2 permit the infrared radiation to enter and leave the White cell.

The Absorption Cell is based upon the work of White (Reference 1). The design requirements call for a total path length of approximately 40" (about 1 meter) in a "small" envelope. The White configuration is illustrated in Figure 16. To achieve these objectives, four basic configurations were analyzed. These four configurations are defined below.

Configuration	M1 Diameter (inches)	M2, M3 Width (inches)	Cell Length (inches)	Number of Passes
1	0.50	0.25	2	20
2	1.00	0.50	2	20
3	1.00	0.50	4	12
4	1.00	0.50	4	20

To determine their effectiveness, the designs were analyzed in terms of aberrations and adjustment sensitivity. As stated in Reference 2, "In a multiple-reflection system, astigmatism can limit the maximum attainable number of passes even more than reflectivity. This aberration causes an increase of the size of each successive image and eventually image overlapping". The alignment problem was alluded to by White in Reference 3, where he states, "With the improved multilayer coatings now available, reflectivity need no longer be limiting, and many more passes would be usable if alignment problems were not prohibitive".

---

1. White, John V., "Long Optical Paths of Large Aperture", J.O.S.A., Vol. 32, May 1942, Pages 285 - 288.

2. Horn, D. and G. C. Pimentel, "2.5-km Low-Temperature Multiple-Reflection Cell", APPLIED OPTICS, Vol. 10, No. 8, August 1971, Pages 1892 - 1898.

3. White, John V., "Very Long Optical Paths in Air", J. Opt. Soc. Am., Vol. 66, No. 5, May 1976, Pages 411 - 416.

Techniques for estimating the aberrations due to astigmatism are described in References 4 and 5 and were used to analyze the performance of the four Absorption Cell configurations listed above.

The results of the aberration analysis are summarized in the following table.

Configuration	M2, M3 f/#	No. of Passes	Vertical Image Plane Size (inches)	Horizontal Image Plane Size (inches)	M1 Diameter (inches)
1	8	20	0.302	0.038	0.500
2	4	20	0.663	0.301	1.000
3	8	12	0.310	0.029	1.000
4	8	20	0.353	0.075	1.000

Configurations 1 and 2 pose potential problems because the two aberrated rows of images occupy such a large percentage of M1's diameter. In order to have room for the input and output windows, M1 must be partially cut away which further compromises these configurations. Configurations 3 and 4, on the other hand, use less than 50% of M1's diameter for the images.

The third configuration will produce the image configuration on M1 that is illustrated in Figure 18.

In addition to consideration of the effects of aberrations on the performance of the absorption cell, consideration must also be given to the need to adjust and align the three mirrors comprising the Absorption Cell. As the number of passes through the Absorption Cell increases, the alignment becomes more critical and the reflection losses increase. Configuration 3 requires only 12 passes and 11 reflections, compared with configurations 1, 2, and 4 which require 20 passes and 19 reflections.

---

4. Reesor, T. R., "The Astigmatism of a Multiple Path Absorption Cell", J. Opt. Soc. Am., Vol. 41, December 1951, Pages 1059 - 1060.

5. Edwards, T. H., "Multiple-Traverse Absorption Cell Design", J. Opt. Soc. Am., Vol. 51, January 1961, Pages 98 - 102.

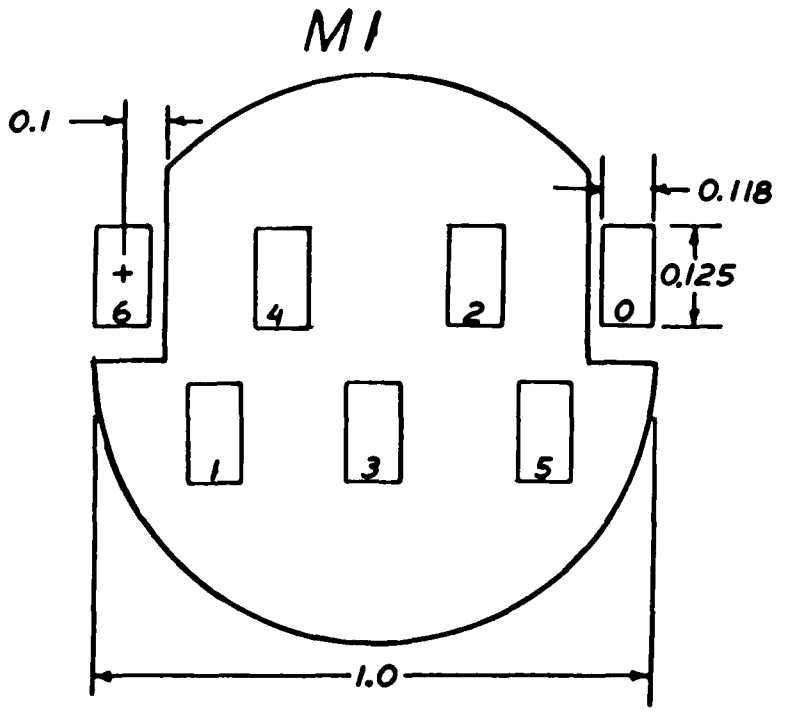

Figure 18. M1 Image Pattern for Selected Absorption Cell Design

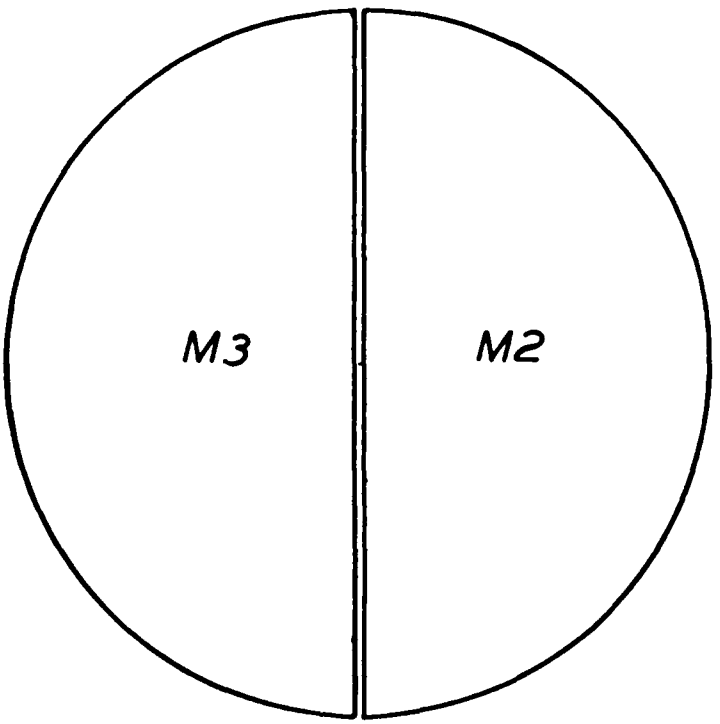

Figure 19. M2 and M3 Mirror Configurations

While the Absorption Cell mirrors could be made with very low loss coatings to reduce reflection losses, the PFLD was constructed with more conventional reflection coatings and hard overcoatings. The reflection losses are somewhat higher, but mirrors can withstand routine handling and cleaning. Using an assumed reflectivity of 96%, configuration 3 produces a reflection loss of 36% compared with a 54% loss for configurations 1, 2, and 4.

The M2 and M3 mirror configurations are illustrated in Figure 19. Both mirrors are made from a common blank to insure matched characteristics.

To place the image surface at the surface of mirror M1 requires provision for axial adjustment of M1 relative to M2 and M3. This adjustment is made by translating M1 relative to M2 and M3.

PFLD System Calibration

The fuel leak detection system was calibrated by varying the concentration of decane in the absorption cell. The cell calibration with decane shown in Figure 7 used the apparatus shown in Figure 16. The flow rates of the pure nitrogen and the nitrogen loaded with decane vapor are controlled separately, thereby producing different concentrations of decane in the absorption cell. The decane partial pressure in the absorption cell, C, is given by

$$C = PV_D/(V_D + V_N) \tag{9}$$

where P is the decane vapor pressure; V_D is the flow rate in the decane flowmeter; and V_N is the flow rate of the nitrogen gas. The decane vapor pressure is 68 ^{o}F = 1700 ppm. Figure 7 shows the calibration of the PFLD using decane. The difference signal obtained with the lock-in amplifier is plotted as a function of the decane concentration in the absorption cell. Measurements were made for decane concentrations from about 30 ppm to 200 ppm. The noise of the system was 0.2 mV, which corresponds to a noise equivalent decane concentration of approximately 1 ppm. The PFLD is adjusted for zero difference signal when there is no absorption in the absorption cell. Thus, the signal is proportional to the decane concentration.

VI. SUMMARY

The objective of this program is to evaluate the spectral correlation technique for measurement of fuel leaks in aircraft. There are two applications: (1) to continously monitor enclosed bays for fuel leaks, and (2) to measure the fuel leak rate after determining that a leak has occurred. The first application requires a rugged, reliable and inexpensive device that can be mounted in aircraft bays and continuously monitor for fuel leaks. The second application could use the same device with a battery attachment for ease in handling by personnel to measure fuel leak rates. The size of the device, including batteries, would be 1" x 2" x 6" and weigh less than 1 pound. It would be particularly useful in situations where the equipment stored in bays makes accessibility to certain regions very difficult and visual identification of leaks practically impossible.

In this Phase I SBIR program, tests were performed with a breadboard spectral correlation device to determine the detection sensitivity and develop a technique for fuel leak measurements. The system determines the presence of the fuel vapor in air by measuring the absorption of infrared radiation by the vapor. Air to be analyzed is sucked into an absorption cell through a 1/4" sampling tube. To detect the presence of a fuel leak in a bay region, the air in the bay would be sampled. Fuel leak rates of less than 0.1 microliters/minute can be readily detected in bays. (This is less than 0.1 the rate to produce a 1/4" spot in 6 minutes with the talc/dye method). The main emphasis of the study was to demonstrate fuel leak rate measurements. Section II predicts the performance of the system for leak rate measurements. The sampling tube is placed over the location of the leak and the increase of the vapor with time gives a direct determination of the leak rate.

Section III treats the measurements made with the device. First the device was calibrated with decane vapor. The output signal is proportional to the decane concentration in the absorption cell. The decane concentration is obtained from the simple relation

Decane concentration (in ppm) = (4.5) Signal (in mV)

The concentration of different fuels would be obtained from a similar formula, but with different calibration constants.

Measurements were made of the leak rate from an aluminum sheet with a 6 mil pinhole. The measurement cycle started by first wiping the surface and then placing the air sampling tube above the leak. The increase in the vapor in the absorption cell was measured and this increase is due to the liquid spreading over the surface. The concentration in the absorption cell increases with time until reaching a steady level, which occurs when the diameter of the liquid layer becomes larger than the diameter of the sampling tube. In section III we show the leak rate to be inversely proportional to the time, t_i, to reach the level portion using the initial slope of the curve. The leak rate for decane is given by the relation

$$\text{Leak rate (in } \mu\ell/\text{min}) = (13\ \mu\ell)/t_i$$

where $t_i = S_p/(dS/dt)$ is in minutes, S is the signal, and S_p is the signal of the level portion. (dS/dt) is the initial slope of the curve.

Thus, by measuring the signal at the level portion and the initial slope, one has a direct determination of the leak rate. It is expected that the level portion can be determined with calibrations and inserted in the software, thus the only requirement is to measure the initial slope to obtain the leak rate. t_i was determined from three leak rate measurements, for leak rates of 3.5, 7.3, and 10 $\mu\ell$/min.

The purpose of this Phase I program was to evaluate methods for detecting fuel leaks in bays and to measure fuel leak rates. More work is required to obtain detailed calibrations for different fuels, and to evaluate the effects of surface curvature and roughness. This report shows that a leak rate method works in the laboratory according to predictions. However, the true utility of this system will only be determined from measurements in the field.

Section IV describes the spectral correlator system and the procedures for selecting the components of the absorption cell and the infrared spectral filters. A breadboard system was assembled, and has a 1 ppm sensitivity for

decane vapor. Fuels have similar absorption coefficients and thus have the same detection sensitivity.

In summary, this program demonstrated that fuel leaks can be detected and leak rate measurements can be made. This device can be made small, rugged, and portable, about 1" x 2" x 6" in size and weighing less than a pound including batteries.

END

6-87

DTIC